Energy Storage and Conversion 2026, 4(1), 4058.
doi: https://doi.org/10.59400/esc4058

Article

Large-scale transferability of a PSO-optimized hybrid energy system: A comparative study of two African regions

Souleymane Kientega*, **Mohammed Ferfra**, **Youssef El Baqqal**

Research Team in Power and Control, Mohammadia's School of Engineering, Mohammed V University in Rabat, Rabat P.B. 765, Morocco

*** Corresponding author:** Souleymane Kientega, souleymane.kientega@research.emi.ac.ma

CITATION

Kientega S, Ferfra M, El Baqqal Y. Large-scale transferability of a PSO-optimized hybrid energy system: A comparative study of two African regions. Energy Storage and Conversion. 2026; 4(1): 4058. https://doi.org/10.59400/esc4058

ARTICLE INFO

Received: 20 February 2026
Revised: 16 March 2026
Accepted: 20 March 2026
Available online: 24 March 2026

Abstract: This study looks at the resilience and cross-region fidelity of a HRES (Hybrid Renewable Energy Systems) across multiple climates in Africa. The study modelled the systems with a PSO (Particle Swarm Optimization) algorithm in MATLAB (Matrix Laboratory). "Large-scale transferability" refers to the system's capacity maintained against tight acceptance criteria. Normalized load curves were used to derive the climate impacts and case studies were in Laâyoune–Sakia El Hamra, Morocco and Ouagadougou, Burkina Faso. They display high adaptability of the systems; a complementarity of winds and solar see a LCOE (Levelized Cost of Energy) of 0.0954 USD/kWh and an annual system cost of $100,039 in Laâyoune–Sakia El Hamra, in Ouagadougou dominates mostly solar, with additional storage requirements, remained very competitive, with LCOE at 0.1014 USD/kWh (+6.3% variance). Both sites achieved similar levels of reliability (Loss of Load Probability, LLP ≈ 0.01) and reduced CO_2 emissions significantly (275.29 tCO_2/yr and 283.13 tCO_2/yr, respectively). LCOE variation was less than 6.5% and LLP variation is less than 0.002, regardless of climate change. These results demonstrate that the flexibility of the methodology employed ensures the maintenance of techno-economic advantages, even in the face of a 45% decrease in wind power potential. Thus, the present paper contributes to the further evolution of HRES design—from an ad hoc narrow-site-specific optimization regime to a scalable, context-sensitive design framework. It also proposes a proven path toward sustainable and affordable renewable energy growth in developing countries.

Keywords: hybrid renewable energy systems; particle swarm optimization; techno-economic optimization; system reliability; transferability analysis

1. Introduction

Having a stable and cheap electricity supply remains a structural issue across much of Africa, even further exacerbated when people live in (semi-) remote and suburban areas, which are unlikely to be easily grid-accessed. In this case, distributed hybrid renewable energy systems (HRES) became a practical solution [1]. Hybrid systems generally consist of some combination of photovoltaic (PV) systems, wind turbines, battery storage and diesel generators as backup. By diversifying the source of power generation and integrating storage into these systems, the volatility of variable sources of generation can be balanced while also reducing operating costs and CO_2 emissions. This analysis allows replicated policy frameworks to be built upon, based on recent advances in CO_2 uptake modelling, Hybrid systems economic evaluation [2–4]. Recent studies show that the economic viability of such systems depends closely on

their technical configuration. This implies that adjustment for optimum is not only a requirement for design, but a necessity for deployment in developing countries [5, 6]. Optimization methods using metaheuristics have become part of the core planning functions of a HRES over the past decade. Particle swarm optimization has been applied to the problem where the search space is a complex nonlinear mixed space very adequately, resolving the size of components under very tight economic and reliable requirements [7–9]. Single-point applications indicate that PSO achieves sufficient saving in cost, with perfect reliability [10–12]. Most applications appear to be isolated spot exercises, so whether the method is effective in certain climate, demand and other profiles will also be effective elsewhere is unresolved.

This lack of portability is the crux of this study; across the African continent there are great disparities in solar irradiation, wind regimes, patterns of demand and institutional context, which result in not only system configuration but also cost structure, storage requirements and potential penetration of renewables varying based on location [13]. Previous work in Libya, Algeria and Sierra Leone for instance has shown that PSO can produce local optima, but that the specific results are dependent on the local context [14–18]. The notion that the PSO framework must be dynamically varied rather than remaining fixed has also not been explored, especially the question of generality across the range of climate types.

To answer this question we are looking at cross regional verification not local tuning. We are trying to find out if one node given the PSO oversight can protect techno-economics selling in two different environments Laâyoune–Sakia El Hamra (stronger coastal winds) and Ouagadougou (stronger solar irradiation) is searching under "wrong" premises or is it truly robust in its performance? Knitting a little tighter certain resource complementarity's and using identical DR's does the hunched short looking node still get us to an LCOE, annual system cost and firming predictability (LLP) do we still get it?

The real value of this comparison is its implications for scalability. Portability is not rebooting the same power system in another area, but instead requires the optimization framework to be adapted to satisfy reliability, cost, and environmental benefits under different boundary conditions. Our work shows that such adaptability is possible when climate/technology constraints are made explicit in the modeling process. In this sense, the innovation of the study is to demonstrate that robustness is derived from adaptive rather than universal design specifications. We clarify the conditions under which hybrid renewable energy system configurations can be optimized across various scenarios and thus enable the development of more resilient, policy-relevant distributed scaling-up planning methods for renewable energy in the context of Africa.

The paper is organized as follows: Section 2 characterizes the selected sites and the optimization framework; Section 3 details the objective functions; Section 4 analyzes the techno-economic results; and Section 5 concludes with implications for future research.

2. Study area characteristics and HRES optimization methodology

2.1. Geographical and climatic characteristics of the study sites

A high level review considering Africa as a whole is not sufficient to compare HRES in general, as geographically and climatically different factors have an influence HRES system design, resource selection, and optimization results [19].To account for this variety, we selected two different use case cities: Ouagadougou, the capital of Burkina Faso, a city center needing a lot of electricity, with solar as a major component, and the Laâyoune–Sakia El Hamra province in the south of Morocco, with its deserts well suited to the use of wind power in addition to solar. Ouagadougou (12°22′12″ N, 1°31′22″ W) is the country's capital economically and politically, covering approximately 219 km^2 and housing nearly 2.77 million residents. The densely packed city at the center, and the space needed to keep electricity flowing to the rapidly growing demand make reliable distributed energy solutions especially important. In comparison, the Laâyoune–Sakia El Hamra area is a sprawling 140,018 km^2 and lies between 23.72° and 27.52° N latitudes and 11.95° and 13.17° W longitudes. With a low population density (approximately 367,758), the siting of hybrid power plants has a lot more space to move around in, but poses quite different logistics challenges. **Figure 1** locations of both sites.

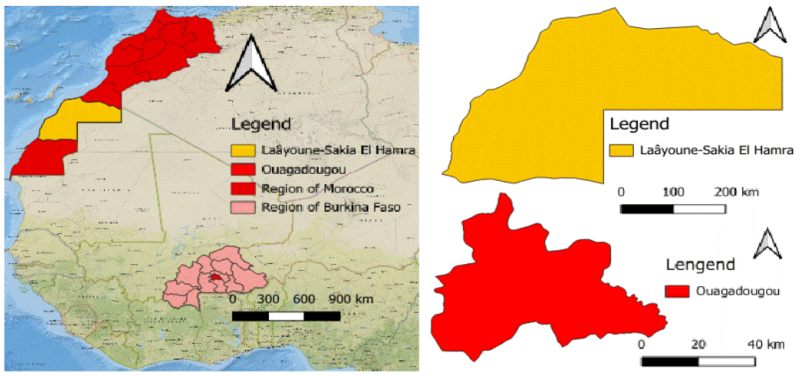

Figure 1. Site location: Laâyoune-Sakia El Hamra region (Morocco); Ouagadougou (Burkina Faso).

For comparability, input meteorological data were normalized. These were collated by NREL and the Global Solar Atlas over multi-year synchronization, and were run through System Consultant Model (SAM) to unify temporal resolution and fill missing values. Cross-validation found a greatly consistent and granular NREL dataset, and were used for global horizontal irradiance GHI and temperature profile forecasts.

There are significant climate differences. For example, in Ouagadougou close to the equator the GHI values are between 4.47 and 5.52 $kWh/m^2/day$, while the temperatures are often above 35 °C, compromising the thermal power of the modules. Wind resources are also scarce, so a solar dominated system design would be appropriate. This is in contrast to the Laâyoune–Sakia El Hamra region with average annual GHI values of over 2,500 kWh/m^2. Wind average speed is also over 8 m/s which accompanies a successful operation of hybrid photovoltaic systems and less dependence

on energy storage.

The wind speed is now a function of the height of the turbine hub. Since our source measurement was taken at a height of 10 m, our simulation at 61 m needs to adjust this information accordingly using the power-law profile as expressed in Equation (2). All meteorological input data generated are summarized in **Figure 2** below, showing the GHI, temperature and adjusted wind speed for Ouagadougou and Laâyoune–Sakia El Hamra. By standardizing our processes in this manner, we know any differences in the optimized results are the result of the climate the data has been taken from rather than the methods we used to prepare our data.

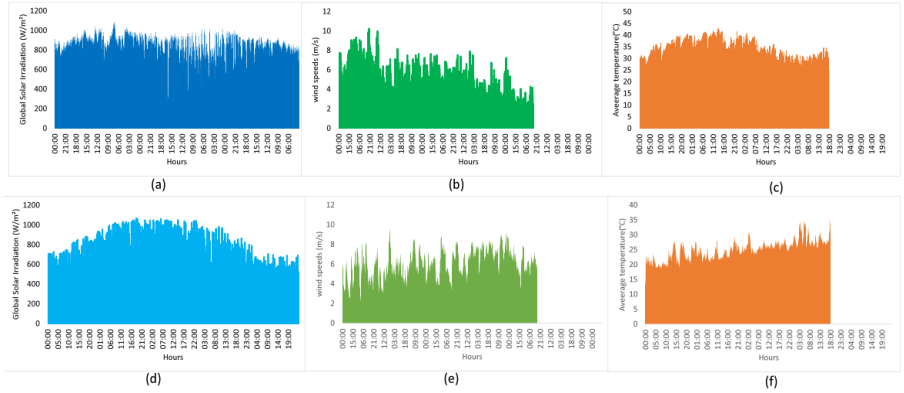

Figure 2. (a–c) Annual meteorological data for Ouagadougou; **(d–f)** Data for Laâyoune-Sakia El Hamra.

2.2. HRES optimization methodology

The optimization approach taken in the present study is a deterministic simulation engine written in MATLAB with a stochastic PSO algorithm attached. This quasi-hybrid discovery of objective orientated system configurations which reach minimum annualized system cost (ASC) with strict adherence to reliability constraints. Unlike the static sizing approaches, this iterative optimization leaves the decision variables to be reviewed at each iteration: photovoltaic capacity, wind turbine rated capacity, battery storage and backup generation. The algorithm iterates to discover techno-economic optima pertinent to the climatic characteristics of each site. The general structure of the system is summarized in **Figure 3.**

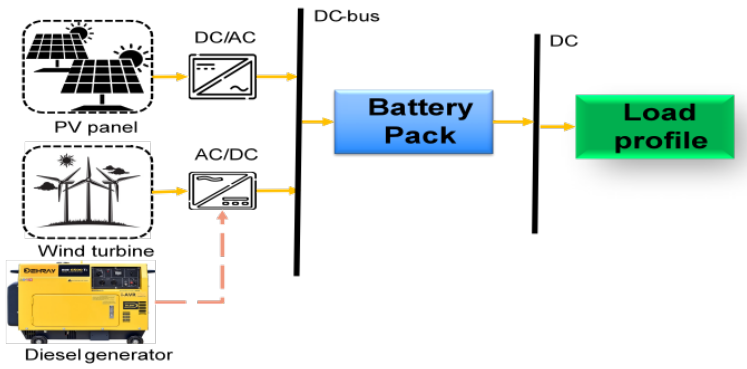

Figure 3. The proposed hybrid system's overall structure.

A key part of the analysis is the validity of demand inputs. Rather than using a standard load curve, time critical load profiles based on aggregated data from 100

modern houses, scaled to include residential, community and small industrial sector loads are created from site specific data to give a baseline daily consumption of 3.76 MWh, and seasonal variation characteristic to each region (represented in **Figure 4**).

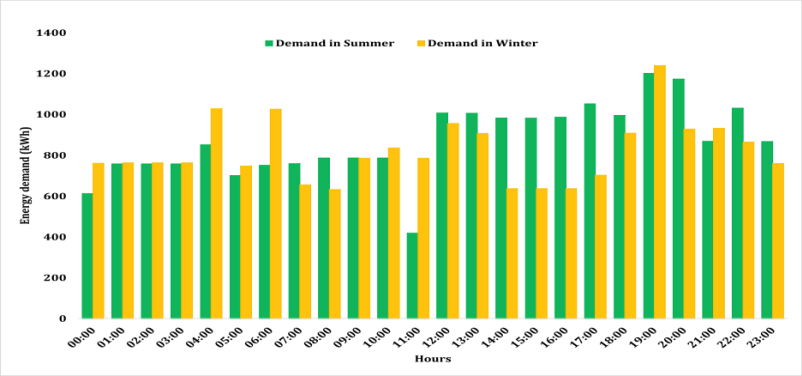

Figure 4. Seasonal fluctuations in hourly load profile.

Using a localized demand model is methodologically important: forcing a cloak of one over all climates would forcibly restrict the optimization process, not expose the real power of the weather.

By pairing high resolution hourly demand data with meteorological data, this means that the differences arise from the real interactions between meteorological and load; this tying of a local demand with a resource whose characteristics are of the climate gives confidence in the consequences of the optimization and reassurance that the conclusion of transferability amongst regions is sound.

2.2.1. Solar resource modeling

PV power (p_{pv}) is calculated by adjusting the rated power based on the GHI index and the temperature deviations of the cells from standard test conditions [20]:

$$p_{pv} = f_{pv} \,.\, k_{pv} \left(\frac{G}{E_{Stc}} \right) [1 + \theta_p \,(T_{cell} \, - T_{stc})] \,, \tag{1}$$

here, f_{pv} is the PV derating factor, k_{pv} is the nominal PV generator capacity (kW), and G is the GHI incident on the PV surface (kW/m^2). T_{cell} is the cell temperature under standard test conditions, and T_{stc} is the reference cell temperature (°C). θ_p is the temperature coefficient of power (%/°C). E_{Stc} is the standard irradiance under test conditions(1 kW/m^2).

2.2.2. Wind resource modeling

Wind energy harvest is estimated using hourly wind speed data translated from the reference measurement height to the turbine hub height through the power-law profile shown in Equation (2). The corrected wind speed is then employed in the turbine power curve model in Equation (3) which implements cut-in, rated and cut-out operating conditions. This way, the simulation can model the approximate nonlinear dependence of wind velocity to electrical yield [13]:

$$U_h = U_{anem} \left(\frac{Z_h}{Z_{anem}} \right)^{\alpha}, \tag{2}$$

where U_h is the wind speed (m/s) at turbine hub height, U_{anem} is the wind speed (m/s)

measured at the anemometer height, Z_h is the hub height (m), Z_{anem} is the anemometer height (m) and α is the power-law exponent. The maximum output of a wind turbine is corrected to account for changes in air density and is given by:

$$P_W = \begin{cases} \eta_w \times P_n \times Nw \times \sum_{t=1}^{8760} \left(\frac{v(t)-v_{cut-in}}{v_r-v_{cut-in}} \right)^3, & v(t) \le v_r \\ \eta_w \times P_n \times Nw, & v_r \le v \le v_{cut-out} \\ 0, & v_{cut-out} \le v(t) \le v_{cut-in} \end{cases}, \tag{3}$$

where η_w is the derivation efficiency, P_n the nominal power, and Nw the number of installed units. Only one input variable is of critical importance, being the wind speed at hub height, $v(t)$, usually inferred from reference measurements using either a logarithmic or power profile.

2.2.3. Diesel generator system

In the hybrid configuration, diesel generators serve as dispatchable backup units. The fuel consumption(L/h, kg/h) is modeled using a linear relationship with a no-load intercept and a load dependent slope [21]:

$$F = f_0 Y_{gen} + f_1 P_{gen}, \tag{4}$$

here, f_0 is the intercept coefficient, f_1 is the fuel curve slope, Y_{gen} is rated generator capacity (kW), and P_{gen} is the electrical output (kW).

Economic evaluation also takes account of both variable costs of fuel and fixed costs associated with operation, maintenance and periodic replacement of the generator:

$$C_{gen,\,fixed} = C_{0\&m,gen} + \frac{C_{rep,\,gen}}{R_{gen}} + f_0 Y_{gen} . C_{fuel,eff}, \tag{5}$$

where $C_{0\&m,gen}$ is the operation and maintenance cost, $C_{rep,\,gen}$ is the replacement cost, R_{gen} is the generator lifetime, and $C_{fuel,eff}$ is given by effective fuel price, which may include penalties for emissions.

2.2.4. Battery storage system

Furthermore, the hybrid system includes a battery bank that stores excess renewable energy, providing electricity when photovoltaic and wind generation fail to meet demand. Battery operation is represented via a state-of-charge (SOC) balance that defines charging and discharging operations as a function of upper and lower state-of-charge limits in Equations (6)–(10). Given excess energy available, charging power [22] is determined by:

$$Pch(t) = Pw(t) + Ps(t) - \frac{Pl(t)}{u_{inv}}. \tag{6}$$

The stored energy is then updated according to:

$$Eb(t) = Eb(t-1) + Ech(t) * n_{bat}. \tag{7}$$

Subject to the constraint:

$$Ech(t) \le Ebmax - Eb(t). \tag{8}$$

Any excess beyond this limit is considered dumped energy. When renewable generation is insufficient to meet demand, the battery discharges according to:

$$Pdch(t) = \left(\frac{Pl(t)}{u_{inv}}\right) - (Pw\,(t) + \ Ps\,(t)) \tag{9}$$

and the state of charge evolves as:

$$Eb(t) = \ Eb(t-1) - \ Edch(t) * \ \lambda \tag{10}$$

while ensuring that the minimum capacity limit Eb_{min} is respected.

2.2.5. Inverters and power converters

Power converters are used to facilitate the exchange of energy between DC fields and AC loads in hybrid RES systems. Thus, the introduction of the power converter makes it possible to feed the wind turbine, and PV array generated electricity into electrical networks or to the consumer.

The inverter capacity is evaluated according to the relationship between the rated power and the maximum load demand considering conversion efficiency, as expressed in Equation (11), to ascertain the minimum inverter rating capable of delivering the peak demand without faulting [22].

$$P_{Inv} \ = \frac{Pl_{max}}{\eta_{Inv}} \tag{11}$$

3. Economic indicators and objective function

The economic assessment of this proposed HRES aims to find configurations that achieve the lowest total system cost while still meeting acceptable reliability and environmental requirements. In practice therefore, this optimization problem is looked at in the following way: there is a techno-economic trade-off when sizing the components of the system to ensure capital costs, operating costs and reliability constraints are balanced. Since hybrid systems contain a number of varying components that interact photovoltaic arrays, wind turbines, batteries, diesel generators and power converters an appropriate objective function needs to be created for assessing the effect of these constituents economically over the project lifetime.

Hybrid systems typically incur high capital costs up front for renewable generation and storage technologies, but tend to have lower overall operating costs compared with fossil-fuel generation once installed. From an economic point of view, this makes accurate sizing even more important as over sizing has the impact of increasing capital expenditure while under sizing increases the possibility that energy deficits will result in a greater proportion of diesel back up required. The optimization procedure combines economic and technical metrics in order to achieve equitable system sizing.

Three main metrics that have been integrated into our optimization procedure are the LLP, LCOE and the ASC. These metrics cover complementary aspects of reliability, cost and sustainability.

Reliability is quantified through LLP [20], defined as:

$$LLP = \frac{\sum_{t=1}^{T}(E_d - E_{plied})}{\sum_{t=1}^{T} E_d}, \tag{12}$$

where E_d signifies the energy demand and E_{plied} the energy delivered at each timestep. Economically, LCOE estimates the average cost of electricity produced across the lifetime of the system [14]:

$$LCOE = \frac{LC_{cost} \times CRF}{\sum_{t=1}^{8760} E_{gen(t)}}, \tag{13}$$

where LC_{cost} is the total life-cycle cost and $E_{gen(t)}$ is the energy generated at each timestep.

The expression for capital recovery factor (CRF) is given as:

$$CRF = \frac{i(1+i)^n}{(1+i)^n - 1}, \tag{14}$$

where *i* is the real interest rate and *n* is the project lifetime.

ASC is the annual system cost inclusive of installed cost, replacement, and maintenance costs [14]:

$$ACS = C_{inst} .CRF_{proj} + \sum_{comp} C_{rep,comp}. \left(\frac{i}{(1+i)^n - 1}\right) + \sum_{comp} C_{O\&M,comp}, \tag{15}$$

where the first term accounts for capital costs; the second replaces the costs by means of a sinking fund factor; the latter combines the annual operation and maintenance cost terms.

Environmental benefits are assessed through avoided CO_2 emissions [20]:

$$AE_{CO2}^{Avoid} = \alpha_{CO2} \times \sum E_{prod}, \tag{16}$$

where α_{CO2} is the emission factor for fossil-fuel generation and E_{prod} the renewable electricity produced.

By including these indicators in the PSO process, the authors discover configurations of the system that are less costly whilst not impacting on its reliability and emissions. These economic parameters can be seen in **Table 1**, such as the investment, replacement and maintenance costs, lifetimes of components, and the real interest rate assumed.

Table 1. Economic parameters adopted for hybrid system components [23,24].

Component	Investment cost	Replacement cost	Maintenance cost	Lifetime (years)
PV array	200 $/kW	—	12 $/kW/year	20
Wind turbine	1,000 $/kW	800 $/kW (0.8 × capital)	30 $/kW/year	20
Battery bank	180 $/kWh	135 $/kWh (0.75 × capital)	2.7 $/kWh/year (0.015 × capital)	12
Diesel generator	175 $/kW	175 $/kW	30 $/kW/year	15
Inverter	171 $/kW	128 $/kW (0.75 × capital)	2.6 $/kW/year (0.015 × capital)	15

3.1. Strengths and limitations of the study

A valuable component of this methodology is that, by embedding site-dependent climatic variability into the economic optimization loop, it allows for a proper

assessment of the transferability of the framework to another part of Africa. The use of high-resolution (hourly) data results in much more credible reliability statistics than if this study was carried on the basis of monthly averaged weather data.

However, we note some limitations. Economic parameters are as of today, and are assumed constant, so no prediction of battery prices or fuel prices under alternative scenarios is included. Likewise, load profiles are aggregate averages, and don't include stochastic load spikes, for example, associated with rapid urban growth or industrial development. The constraints mean that, while the results should be very useful for policy planning, they can be treated as indicative optima until confirmed with live tracked real data.

3.2. Particle swarm optimization (PSO) algorithm

The PSO is also a population-based metaheuristic determined by the way in which a number of individuals exhibit a coordinated behavior whilst acting as a group, such as bird flocking or fish schooling. Each particle in this study represents a configuration of the hybrid system with the five decision variables selected to represent the main design parameters. Particles move through a N-dimensional search space and update their new position based on two reference points, the particle's own best solution ($pbest$) and the best solution identified by the swarm ($gbest$). By use of this social behavior the swarm is lead toward highly competitive solutions, but the trajectory is still determined by the domain of the objective function.

Each particle updates its velocity and its position using classical PSO technique [25]:

$$v_i^{k+1} = wv_i^k + c_1 r_1 \left(pbest_i - x_i^k \right) + c_2 r_2 \left(gbest - x_i^k \right), \tag{17}$$

$$x_i^{k+1} = x_i^k + v_i^{k+1}. \tag{18}$$

The optimization problem is framed, as a weighted multi-objective function:

$$\min_x F(x) = w_1 C_{tot} + w_2 LLP + w_3 \left(1 - \eta_{sys}\right) \; with \; \sum w_i = 1, \tag{19}$$

where C_{tot} is the total cost of the system for the year, *LLP* the loss of load probability and η_{sys} the efficiency of the system.

The PSO procedure was executed with a swarm of 40 particles for 100 iterations. The inertia weight was decreased from 0.9 to 0.2, providing balance between exploration and exploitation, while acceleration coefficients were set to c1 = c2 = 2 used in many more recent examples in the literature to ensure stability.

4. Results and discussion

The objective of this work is to design and validate a transferable and flexible optimization engine for HRES ensuring reliable and cost-effective operation across a wide range of climates throughout Africa. Where traditional design optimization

studies end with the optimization of one site, we prove the concept of large-scale transferability. By 'transferability' we mean quantitatively how the proposed PSO algorithm would 'know' how to resize a site (PV, Wind, Battery, Diesel), such that LLP < 1% remains throughout and LCOE lowers, across a very different renewable resource profile, without structural or logic level changes to the control algorithm.

This simulation environment was created in MATLAB, with high-quality meteorological data as described in Subsection 2.1 used as inputs for model cities Ouagadougou (Burkina Faso) and Laâyoune (Morocco). The deterministic load modelling against stochastic renewables generation profiles were solved in a multi-objective PSO algorithm minimizing both LCOE and LLP.

4.1. Assessment of convergence behavior and reliability

The trajectories of the objective function convergence for the two studied sites are shown in **Figure 5**, with **Figure 5a** corresponding to Ouagadougou and **Figure 5b** to Laâyoune–Sakia El Hamra. The rapid decrease in the objective function is observed during the first iterations in both cases, followed by a much calmer decrease which remains stable as the swarm approaches a decent solution. This indicates the optimization process is numerically stable, and that cheap configurations will tend to be found in a smaller number of turns.

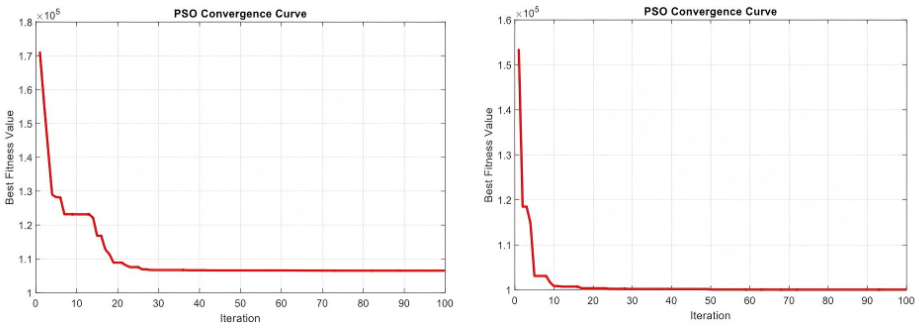

(**a**) (**b**)

Figure 5. Convergence curves of the PSO objective function for **(a)** Ouagadougou; **(b)** Laâyoune–Sakia El Hamra.

When analyzing the two curves, there are subtle differences in the way the systems settle. Laâyoune–Sakia El Hamra seems to settle earlier, highlighting the better complementarity of the wind and solar resources there. Ouagadougou appears to take a few more steps to get to the minimum, a function of its solar dominance relying more on batteries and backup generation to meet its reliability requirements.

The periods during which the LLP rises above the critical reliability threshold are delineated in **Figure 6**. In **Figure 6** we show such periods for Ouagadougou and Laâyoune–Sakia El Hamra, respectively. Despite overall low LLP values, at times the risk briefly escalates, mainly when renewable generation falls off and the stored energy levels are not sufficient to maintain the demand. For Ouagadougou, this occurs in the dark hours when solar irradiation is low and the wind generation is weak, necessitating battery discharges and the occasional use of diesel generations. For Laâyoune–Sakia El Hamra, the high-LLP periods are rarer, mainly because the wind is persistent, and

thus has a continuous and least intermittent contribution to the generation mix.

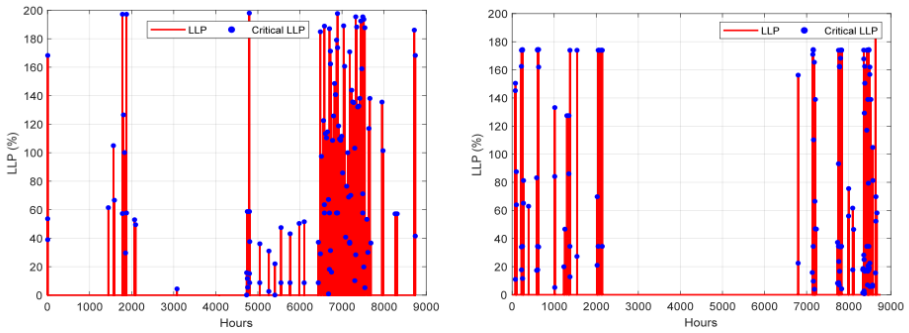

Figure 6. Hourly loss of load probability distribution for **(a)** Ouagadougou; **(b)** Laâyoune–Sakia El Hamra.

4.2. Short and long-term operational energy balance

A week of dispatch of the optimized systems, typical of their short run behavior is summarized in **Figure 7**. Although this figure does not capture the extensive variability within a year it illuminates the interaction between renewables, storage and backup generation.

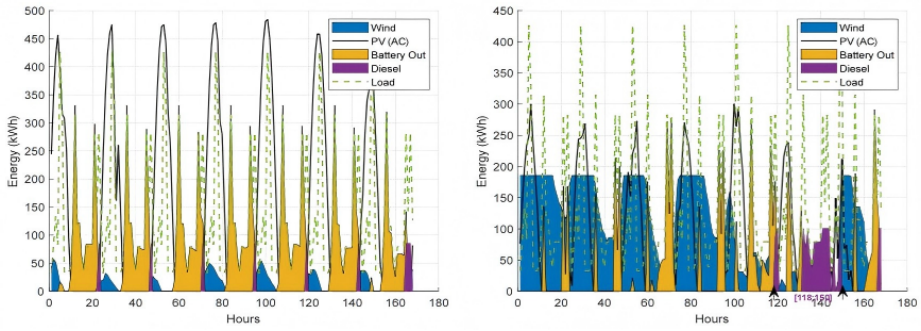

Figure 7. Hourly energy balance during a representative week in January for **(a)** Ouagadougou; **(b)** Laâyoune–Sakia El Hamra.

In Ouagadougou, the comparably greater volume of daytime photovoltaic generation is offset by lower production at other times of the day, with the effect of the wind helping remove some pressure from the batteries at night. When neither renewable source is supplying sufficient current, the diesel generator starts up to maintain the reliability of supply. In Laâyoune–Sakia El Hamra, stronger and more even wind resources supplement the production of solar PV during the daytime, leading to a smoother generation profile overall and fewer batteries and diesel interventions.

Figure 8 shows the results obtained when implementing the hourly simulation over the entire year (8,760 h). Ouagadougou: the system is fairly solar powered, generating 1.23 GWh/yr (about 62% of demand) from photovoltaics, 11% from wind, and 26% of its internal needs are met via battery storage. Laâyoune–Sakia El Hamra is much more balanced, wind accounts for nearly 1.10 GWh (about 53%) of the supply, with solar providing 0.75 GWh. Because the wind generation is relatively constant

throughout the year, relatively little battery storage is used by comparison with the Ouagadougou case.

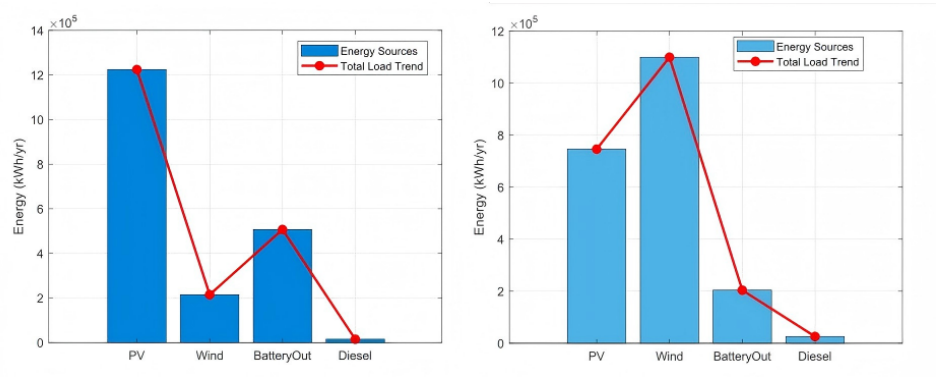

Figure 8. Annual energy and total load trends for **(a)** Ouagadougou; **(b)** Laayoune-Sakia El Hamra.

4.3. Optimal configuration of the system and seasonal energy balance

The sizes of the components that turned out to be optimal for each site are presented in **Table 2**. As expected, notable differences between the two hybrid systems arose due to the differing availability of the renewable energies. In the case of the Laâyoune–Sakia El Hamra region, the optimized solution is wind dominant, with a number of 174 wind turbines and 422 photovoltaic modules. The demand for batteries is in this case moderate (1,435), which suggests that the natural complementarity of those two sources reduces the need for extensive back-up battery energy storage.

Table 2. Optimization results and performance comparison of HRES configurations in Ouagadougou and Laâyoune–Sakia El Hamra.

Study sites	Design	PV unit	Wind unit	Battery unit	Diesel unit	Diesel starts/year
Laayoune-Sakia El Hamra(Morocco)	PV/WT/DG/Bat	422	174	1,435	109	81
Ouagadougou(Burkina Faso)		627	60	2,075	85	101

By contrast, the preferred system configuration in Ouagadougou is highly solar-dependent at 627 photovoltaic modules and only 60 wind turbines. Given the limited wind resource this means a much larger battery storage capacity (2,075 units) is required to cater for fluctuations in solar generation and utility of the system. However, the demand for diesel backup power is minimal in both cases.

The variation of energy consumption as each month becomes a distinct curve is shown in **Figure 9**, which also reflects seasonal variations. In Ouagadougou, generation by photovoltaics predominates throughout the year, with wind power only providing additional energy, so that the system is more dependent on battery storage to offset short term changes, while seasonal variations in the Laâyoune–Sakia El Hamra region are more of a balance—uninterrupted generation from wind and solar power for most months supporting itself, smoothing out variations, and reducing dependence on energy storage.

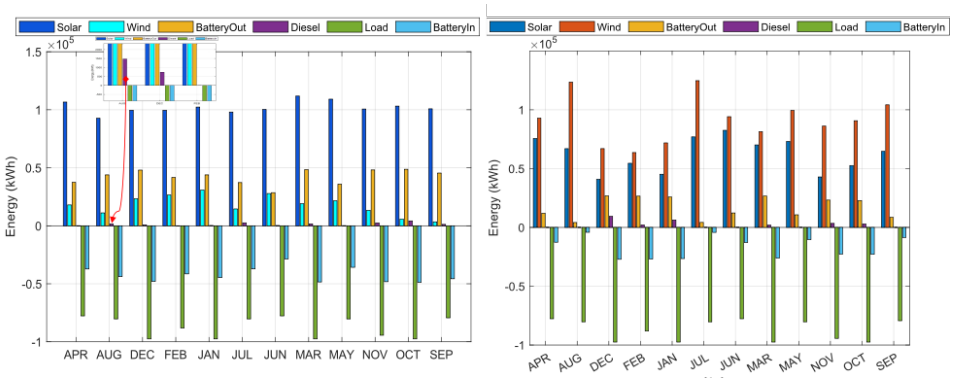

(**a**) (**b**)

Figure 9. Monthly energy generation by source for **(a)** Ouagadougou; **(b)** Laayoune-Sakia El Hamra.

4.4. Techno-economic performance of the optimized systems

Optimization framework yielded two families of architectures, tuned locally to resource conditions and strictly reliability constrained (LLP < 1%). Aspects of techno-economic performance are summarized in **Table 3** emphasizing the way resources shape capital and opex allocation.

Table 3. Breakdown of CAPEX for each system component and key performance indicators.

Study sites	PV CAPEX (USD/yr)	Wind CAPEX (USD/yr)	Battery CAPEX (USD/yr)	Diesel CAPEX (USD/yr)	Inverter CAPEX (USD/yr)	ASC (USD/yr)	LCOE (USD/kWh)	CO_2 (t)	LLP
Laayoune-Sakia El Hamra (Morocco)	13,266.31	25,256.11	35,840.93	17,214.97	8,460.92	100,039.24	0.0954	275.29	0.00995
Ouagadougou (Burkina Faso)	19,719.44	8,599.26	51,803.76	13,652.48	12,528.37	106,303.30	0.1014	283.13	0.00969

Laâyoune–Sakia El Hamra has sufficient wind that a diversified generation mix has better economics. In total, the system has an ASC of USD 100,039.24 and an LCOE of USD 0.0954/kWh. Capital expenditure is split between different technologies, with wind turbines accounting for 25.2% and batteries 35.8%. This combination highlights the advantages of high capacity factor, where power is available at an elevated degree at all times, reducing the need for maximally oversized storage and allowing capital to be distributed more evenly.

In the case of Ouagadougou, the situation is significantly solar-dependent because the wind potential is constricted. Although this configuration is reliable, the greater dependency on it (which warrants a larger battery bank to see us through diurnal intermittency and seasonal cloud cover) means battery CAPEX rises to 48.7% of total investment (USD 51,803.76/year), so that the ASC is USD 106,303.30 and the LCOE is USD 0.1014/kWh. Both are reliable (we have LLP 0.00995 for Laâyoune–Sakia El Hamra, and 0.00969 for Ouagadougou, which is well below the 1% threshold). Both see CO_2 emissions kept relatively low (~275–283 t/year) too, so deep decarbonization is possible in all circumstances, irrespective of technology mix, as long as it is sized appropriately.

Table 4 also presents a breakdown of costs through robustness indices, showing what fraction of the total annualized cost each component CAPEX constitutes. As can be seen here there is much to trade-off; in Ouagadougou, which has relatively low wind resource, the “storage penalty” increases the proportion of costs due to batteries

(by 13% compared to Laâyoune–Sakia El Hamra). At the same time, the amount of diesel fuel used is lower in Ouagadougou (3,976 L/yr vs. 6,883 L/yr in Laâyoune), so the added battery bank provides a better cushion against supply shortages and increases the frequency of time which not starting generators; despite its added CAPEX.

Table 4. Robustness indices of economic parameters for CAPEX by component.

Study site	PV share (%)	Wind share (%)	Battery sare (%)	Diesel ssare (%)	Inverter share (%)	Diesel fuel (L/yr)	CRF
Laâyoune	13.4	25.2	35.8	17.0	8.5	6,883.6	0.0872
Ouagadougou	18.6	8.1	48.7	12.8	11.8	3,976.2	0.0872

4.5. Novelty, contributions, and critical assessment

This work adds to the accessible HRES literature by looking not at site-specific optimums, but transferability of methodology. Instead of focusing on a specific site, previous researchers consider "what if" scenarios. Here we make a closed comparison of Laâyoune (North Africa) and Ouagadougou (West Africa) using identical demand profiles and economic figures and isolating the effect of endowment of resources. Seeing how the proposed PSO dynamically resizes the components according to climate and resource endowments: Laâyoune followed the wind with limited storage (≈10.6%), Ouagadougou led with solar-storage dominated (≈25.9%) architecture. The resulting LCOE's (0.0954 and 0.1014 USD/kWh respectively) shows that near-total RES penetration is viable in much of Africa, rather than substantial diesel reliance being a given overall.

The key contribution here is in providing methodological rigor of metrics such as LCOE stability, reliability compliance and evidence of component adaptation which give researchers/designers a means of further assessing other optimization algorithm components in a reproducible manner beyond the one-off individual case studies. This assessment is further developed with quality controlled NREL meteorological data, a transparent tuning of PSO's parameters, and based on multi-metric assessment of the LLPs distribution and the CO_2 reductions.

That said, a few caveats. The constant load profile, useful as it may be for isolating the effects of the resource, somewhat obscures normal demand variability. Static economic parameters and simple battery degradation metrics potentially understate costs in more landlocked areas and high-cycling locations, and the two-site coverage although clearly distinct enough to be sliced into a few scenarios doesn't enter every regional and climate zone on the continent.

5. Conclusion

This study demonstrated the large-scale transferability of a PSO-harmonized hybrid renewable energy system across two significantly different African locations; Laâyoune–Sakia El Hamra (Morocco) and Ouagadougou (Burkina Faso). In moving beyond single-site case studies we provided a quantitative definition of "large-scale transferability", namely the ability of the system to maintain performance against defined acceptance criteria. To assess the extent to which the geographic disparity of sites add variability a common demand profile was imposed; the outcome of our

sensitivity analysis demonstrated that this approach verifies climatic agencies, with minimal error (<1.5%) on final costs allowing for the relative impact of resource characteristics to be compared directly.

The numerical results further testify to these convictions. In Laâyoune, the strong wind–solar complementarity available produces the lowest LCOE (0.0954 USD/kWh), the lowest ASC (100,039 USD/yr) and the largest CO_2 reduction (275.29 t). In Ouagadougou, the algorithm rebalances: the storage-to-generation ratio is different so there's no sense simply iterating on the model solution and getting back the previous 'optimal' solution. A gentle incline Up a rut therefore exists, simply moving up not only doesn't 'lose its way' but gathers support along that trajectory entering in response. The LCOE is now marginally increased (0.1014 USD/kWh, 6.3%), for a small cost to ASC (106,303 USD/yr) and even smaller to net emissions saved (283.13 t). Reliability standards (LLP ≈ 0.01) remain unchanged. Overall, the performance metrics make it clear the methodology is not blindly copying, but instead dynamically reallocating contextually pertinent levers, preserving economic viability and operational stability. ΔLCOE in Laâyoune less than 6.5%, ΔLLP of 0.002 or less, holds true regardless of climatic variability.

We show HRES optimization frameworks are inherently decoupled from geography. Our results show one set of code can promote techno-economic viability across regions with varying, wind–solar regimes, transitioning the HRES design paradigm from isolated project to scalable regional energy planning.

These results therefore provide direction to policymakers and engineers seeking to roll out established resilient microgrids to developing countries and should favor adopting locally calibrated adaptive PSO based methods, which currently outweigh standardized component sizing. Future work can further this analysis to expand the transferability results to a wider range of at least ten sites, as well as develop a more representative set of robustness indices. Additionally, contributing models on incorporating demand response in real-time and the validation of new storage technologies such as green hydrogen to help enable a full generalizable rollout of large scale renewables across Africa.

Author contributions: SK: conceptualization, methodology, formal analysis, writing—original draft preparation; MF: supervision, investigation, project administration; YEB: writing—review and editing, validation. All authors have read and agreed to the published version of the manuscript.

Funding: This work received no external funding.

Institutional review board statement: Not applicable.

Informed consent statement: Not applicable.

Data availability statement: The data supporting the findings of this study are available from the corresponding author upon reasonable request. No publicly archived datasets was used or generated. Requests will be considered in accordance with applicable ethical and legal restrictions.

Conflict of interest: The authors declare no conflict of interest.

References

1. Nyarko K, Whale J, Urmee T. Drivers and challenges of off-grid renewable energy-based projects in West Africa: A review. Heliyon. 2023; 9(6): e16710. doi: 10.1016/j.heliyon.2023.e16710
2. Ebrahimi A, Ghorbani B, Taghavi M. Novel integrated structure consisting of CO_2 capture cycle, heat pump unit, Kalina power, and ejector refrigeration systems for liquid CO_2 storage using renewable energies. Energy Science & Engineering. 2022; 10(8): 3167–3188. doi: 10.1002/ese3.1211
3. Soonmin H, Taghavi M. Solar Energy Development: Study Cases in Iran and Malaysia. International Journal of Engineering Trends and Technology. 2022; 70(8): 408–422. doi: 10.14445/22315381/IJETT-V70I8P242
4. Afrouzy ZA, Taghavi M. Thermo-economic analysis of a novel integrated structure for liquefied natural gas production using photovoltaic panels. Journal of Thermal Analysis and Calorimetry. 2021; 145(3): 1509–1536. doi: 10.1007/s10973-021-10769-4
5. Taghavi M, Lee CJ. Development of a novel hydrogen liquefaction structure based on liquefied natural gas regasification operations and solid oxide fuel cell: Exergy and economic analyses. Fuel. 2025; 384: 133826. doi: 10.1016/j.fuel.2024.133826
6. Taghavi M, Lee CJ. Development of novel hydrogen liquefaction structures based on waste heat recovery in diffusion-absorption refrigeration and power generation units. Energy Conversion and Management. 2024; 302: 118056. doi: 10.1016/j.enconman.2023.118056
7. Mquqwana MA, Krishnamurthy S. Particle Swarm Optimization for an Optimal Hybrid Renewable Energy Microgrid System under Uncertainty. Energies. 2024; 17(2): 422. doi: 10.3390/en17020422
8. Mehallou A, M'hamdi B, Amari A, et al. Optimal multiobjective design of an autonomous hybrid renewable energy system in the Adrar Region, Algeria. Scientific Reports. 2025; 15(1): 4173. doi: 10.1038/s41598-025-88438-x
9. Znati I, Ferfra M, Bouaddi A, et al. TID Controller for Load Frequency Control in Multi-Area Interconnected Systems with High Renewable Energy Penetration Using an Improved Grey Wolf Algorithm. In: Proceedings of the 2025 5th International Conference on Innovative Research in Applied Science, Engineering and Technology (IRASET); 15 May 2025; Fez, Morocco. pp. 1–8. doi: 10.1109/IRASET64571.2025.11008173
10. Mulenga E, Kabanshi A, Mupeta H, et al. Techno-economic analysis of off-grid PV-Diesel power generation system for rural electrification: A case study of Chilubi district in Zambia. Renewable Energy. 2023; 203: 601–611. doi: 10.1016/j.renene.2022.12.112
11. Yamegueu D, Nelson HT, Boly AS. Improving the performance of PV/diesel microgrids via integration of a battery energy storage system: the case of Bilgo village in Burkina Faso. Energy, Sustainability and Society. 2024; 14(1): 48. doi: 10.1186/s13705-024-00480-1
12. El Hafdaoui H, Khallaayoun A, Al-Majeed S. Renewable energies in Morocco: A comprehensive review and analysis of current status, policy framework, and prospective potential. Energy Conversion and Management: X. 2025; 26: 100967. doi: 10.1016/j.ecmx.2025.100967
13. Marocco P, Ferrero D, Lanzini A, et al. The role of hydrogen in the optimal design of off-grid hybrid renewable energy systems. Journal of Energy Storage. 2022; 46: 103893. doi: 10.1016/j.est.2021.103893
14. Yahya W, Saied KM, Nassar A, et al. Optimization of a hybrid renewable energy system consisting of a of PV/wind turbine/battery/fuel cell integration and component design. International Journal of Hydrogen Energy. 2024; 94: 1406–1418. doi: 10.1016/j.ijhydene.2024.11.187
15. Fodhil F, Hamidat A, Nadjemi O. Potential, optimization and sensitivity analysis of photovoltaic-diesel-battery hybrid energy system for rural electrification in Algeria. Energy. 2019; 169: 613–624. doi: 10.1016/j.energy.2018.12.049
16. Konneh D, Howlader H, Shigenobu R, et al. A Multi-Criteria Decision Maker for Grid-Connected Hybrid Renewable Energy Systems Selection Using Multi-Objective Particle Swarm Optimization. Sustainability. 2019; 11(4): 1188. doi: 10.3390/su11041188
17. Taghavi M, Salarian H, Ghorbani B. Thermodynamic and exergy evaluation of a novel integrated hydrogen liquefaction structure using liquid air cold energy recovery, solid oxide fuel cell and photovoltaic panels. Journal of Cleaner Production. 2021; 320: 128821. doi: 10.1016/j.jclepro.2021.128821
18. Ghorbani B, Salehi G, Ebrahimi A, et al. Energy, exergy and pinch analyses of a novel energy storage structure using post-combustion CO_2 separation unit, dual pressure Linde-Hampson liquefaction system, two-stage organic Rankine

cycle and geothermal energy. Energy. 2021; 233: 121051. doi: 10.1016/j.energy.2021.121051
19. Matera N, Mazzeo D, Baglivo C, et al. Energy Independence of a Small Office Community Powered by Photovoltaic-Wind Hybrid Systems in Widely Different Climates. Energies. 2023; 16(10): 3974. doi: 10.3390/en16103974
20. Kientega S, Ferfra M, Youssef EB. Optimization of a Hybrid PV–Wind–Battery System for Sustainable Energy Production. In: Proceedings of the 2025 IEEE 8th Congress on Information Science and Technology (CiSt); 4 October 2025; Marrakech, Morocco. pp. 260–267. doi: 10.1109/CiSt65886.2025.11224228
21. Basem A, Elbarbary ZMS, Atamurotov F, et al. Optimal sizing of PV/wind/diesel generator/battery hybrid system for supplying electrical vehicle charging station under different load demands in Saudi Arabia. International Journal of Low-Carbon Technologies. 2024; 19: 2522–2539. doi: 10.1093/ijlct/ctae190
22. Samy MM, Güven AF. Optimal dimensioning of grid-connected PV/wind hybrid renewable energy systems with battery and supercapacitor storage: A statistical validation of meta-heuristic algorithm performance. Scientific Reports. 2025; 15(1): 45658. doi: 10.1038/s41598-025-28234-9
23. Akhtari M, Karlström O. Role of wind speed and solar irradiation on the cost of medium-sized off-grid hybrid renewable energy systems under challenging weather conditions. Energy Conversion and Management: X. 2025; 27: 101163. doi: 10.1016/j.ecmx.2025.101163
24. Reuchlin S, Joshi R, Schmehl R. Sizing of Hybrid Power Systems for Off-Grid Applications Using Airborne Wind Energy. Energies. 2023; 16(10): 4036. doi: 10.3390/en16104036
25. Sulaiman AT, Bello-Salau H, Onumanyi AJ, et al. A Particle Swarm and Smell Agent-Based Hybrid Algorithm for Enhanced Optimization. Algorithms. 2024; 17(2): 53. doi: 10.3390/a17020053